JOURNAL OF Materials CHEMISTRY

Spectroscopic characterization of (BEDT-TTF)$_2$[Pt(S$_2$C$_4$O$_2$)$_2$] charge density wave ground state

Matteo Masino,[a] Giovanni Visentini,[a] Carlo Bellitto[b] and Alberto Girlando*[a]

[a]*Dip. Chimica Generale ed Inorganica, Chimica Analitica e Chimica Fisica, Parma University, I-43100 Parma, Italy. E-mail: girlando@ipruniv.cce.unipr.it*
[b]*Istituto di Chimica dei Materiali del CNR, Area della Ricerca di Roma, CP10, I-00016 Monterotondo Staz., Roma, Italy*

Received 1st March 1999, Accepted 18th May 1999

We report a detailed spectroscopic characterization of the charge transfer (CT) complex between bis(ethylendithio)tetrathiafulvalene (BEDT-TTF) and bis(dithiosquarate)platinate(II), (BEDT-TTF)$_2$[Pt(S$_2$C$_4$O$_2$)$_2$]. In this complex BEDT-TTF dimers are separated by the [Pt(S$_2$C$_4$O$_2$)$_2$]$^{2-}$ anions, forming a quasi-one-dimensional stack. We show that the stack structure is stabilized by CT between BEDT-TTF dimers *and* between BEDT-TTF and [Pt(S$_2$C$_4$O$_2$)$_2$]. Two CT transitions, polarized along the stack axis, are identified in the optical spectra. Furthermore, the average charge on the molecules is not a multiple integer, and the amplitude of the intrinsic ground state charge density wave (CDW) can be represented as: …[Pt(S$_2$C$_4$O$_2$)$_2$]$^{1.8-}$BEDT-TTF$^{0.9+}$BEDT-TTF$^{0.9+}$[Pt(S$_2$C$_4$O$_2$)$_2$]$^{1.8-}$… The optical spectra polarized along the (BEDT-TTF)$_2$[Pt(S$_2$C$_4$O$_2$)$_2$] stack are well reproduced by a semiempirical model which takes into account the coupling of BEDT-TTF molecular vibrations with the CT electrons (e–mv coupling). Under pressure, (BEDT-TTF)$_2$[Pt(S$_2$C$_4$O$_2$)$_2$] undergoes two distinct phase transitions in the ranges 1–1.6 and 2.2–2.5 GPa, the first involving a stack distortion.

1 Introduction

Bis(ethylenedithio)tetrathiafulvalene (BEDT-TTF) is one of the most important electron donors in the field of synthetic metals. Over thirty of its salts with closed-shell anions exhibit superconducting properties, and others behave as metals down to very low temperatures.[1,2] Subtle interplay between superconducting and magnetically ordered states has been observed.[3] Furthermore, interesting electric and magnetic properties have been observed in BEDT-TTF salts containing magnetic transition metal anions or magnetic inorganic clusters.[4] Another interesting investigation pathway is the combination of BEDT-TTF with open shell transition metal anions, such as the metal–dithiolene complexes, which can contribute to the electric properties of the salts.[5] In most systems BEDT-TTF networks are separated from those of the transition metal anions. A novel and so far little explored possibility is to use planar transition metal anions of dimensions comparable to those of BEDT-TTF, so that the cation and anion units can be more closely packed together.

Following the latter route, several complexes of BEDT-TTF with bis(dithiosquarate)metalate [M(S$_2$C$_4$O$_2$)$_2$], hereafter [M(dts)$_2$], have been recently prepared.[6,7] However, only the crystal structures and the electrical properties of these salts have been reported. Here, we present a detailed spectroscopic characterization of the first compound of the series, (BEDT-TTF)$_2$[Pt(dts)$_2$]. In this crystal, (BEDT-TTF$^+$)$_2$ dimers alternate with [Pt(dts)$_2$]$^{2-}$ along the *b* crystallographic direction,[6] forming what might be considered a sort of regular mixed stack.[8] We unambiguously prove the presence of direct charge-transfer (CT) interaction between adjacent BEDT-TTF and [Pt(dts)$_2$] units. We find that the average charge on the cation is sligthly less than one, and identify in the optical spectra two CT transitions, one between two adjacent BEDT-TTF units, and the other between BEDT-TTF and the [Pt(dts)$_2$] anion. We show that the (BEDT-TTF)[Pt(dts)$_2$] stack can be modeled as a trimerized stack with a site charge density wave (s-CDW) distortion, as for instance found in Cs$_2$(TCNQ)$_3$.[9] We also study the effect of temperature and pressure on the s-CDW amplitude, and show that under pressure (BEDT-TTF)$_2$[Pt(dts)$_2$] undergoes a phase transition implying a distortion of the stack, *i.e.* bond-CDW (b-CDW) overlapping the intrinsic ambient pressure s-CDW.

2 Experimental

(BEDT-TTF)$_2$[Pt(dts)$_2$] was prepared by an electrocrystallization technique as previously described.[6] Dark, needle-like crystals of a few tenths of a mm wide were obtained. The synthesis of the potassium salt of the anion, K$_2$[Pt(dts)$_2$]·2H$_2$O, was performed following the literature method.[10]

Polarized absorption and normal incidence reflectance spectra of (BEDT-TTF)$_2$[Pt(dts)$_2$] single crystals in the 600–9000 cm^{-1} spectral region were obtained on a Bruker IFS66 FT spectrometer equipped with a KBr beamsplitter. Globar and tungsten lamp sources and wire grid KRS5 and Polaroid HR type polarizers were used for mid- and near-IR measurments, respectively. The spectrometer was equipped with a Bruker A590 infrared (IR) microscope and mercury cadmium telluride (MCT) detector. The reflectance data were normalized to the reflectance of a high quality silver mirror. Care is required to focus the microscope on a smooth portion of the sample, so that the spectra reproduce the *absolute* reflectance of the crystal. Polarized reflectance spectra were also measured in the 600–18000 cm^{-1} spectral range on a mosaic of parallel (BEDT-TTF)$_2$[Pt(dts)$_2$] needles, using a Harrick Seagull reflectance accessory. In the region 12000–18000 cm^{-1} a quartz beamsplitter, Si detector and Polaroid HN7 polarizer were used. Unpolarized absorption spectra in the 400–600 cm^{-1} region were obtained from a thin layer of powder deposited on a KBr disk, using a DTGS-CsI detector. The absorption spectra of K$_2$[Pt(dts)$_2$] powders were measured as Nujol mulls between 400 and 4000 cm^{-1}. Liquid-nitrogen temperature IR spectra under a microscope were obtained with a Linkam HFS91 cold stage. High pressure polarized IR absorption spectra were recorded on a single crystal with a custom designed diamond anvil cell (DAC) which fits under the microscope. The pressure was calibrated against ruby luminescence.[11]

The samples for the Raman measurments were prepared by gently pressing a microcrystalline powder of (BEDT-TTF)$_2$[Pt(dts)$_2$] diluted in KBr onto a KBr disk. The Raman spectra were recorded with a multichannel triple spectrograph (Jobin-Yvon S3000) equipped with a CCD detector. The Ar^+ laser (Coherent) line at 488.0 nm was focused by a cylindrical lens to a slit image 150 mm wide. The laser power was kept as low as 15 mW (room temperature) and 50 mW (low temperature) in order to avoid sample heating and degradation. Low-temperature (*ca.* 20 K) Raman spectra were recorded on samples mounted in closed-cycle refrigerators (CTI Cryodyne mod.21 and mod.22C).

3 Results

3.1 Ambient conditions optical spectra

Polarized reflectance spectra of (BEDT-TTF)$_2$[Pt(dts)$_2$] in the region 600–18000 cm^{-1} are shown in Fig. 1 (note the logarithmic wavenumber scale). The radiation was polarized with the electric field parallel (∥) or perpendicular (⊥) to the (BEDT-TTF)$_2$[Pt(dts)$_2$] stack axis, *b* in the monoclinic unit cell.[6] The electronic transitions observed at 11000 cm^{-1} (∥ polarization) and at 12500 cm^{-1} (⊥ polarization) correspond to localized (excitonic) transitions of BEDT-TTF$^+$,[12] whereas the ⊥ band around 17000 cm^{-1} can be attributed to a localized transition of the bis(dithiosquarate)platinate(II) anion.[6] The two strong transitions around 4500 and 7000 cm^{-1} are not observed in the monomeric cation or anion spectra,[12] and are clearly identified as two CT transitions, one between two nearby BEDT-TTF in the stack, and the other between BEDT-TTF and [Pt(dts)$_2$] moieties.

To perform a Kramers–Kronig transformation we have extrapolated the reflectance data to zero frequency with a constant value equal to that measured at the lowest frequency,

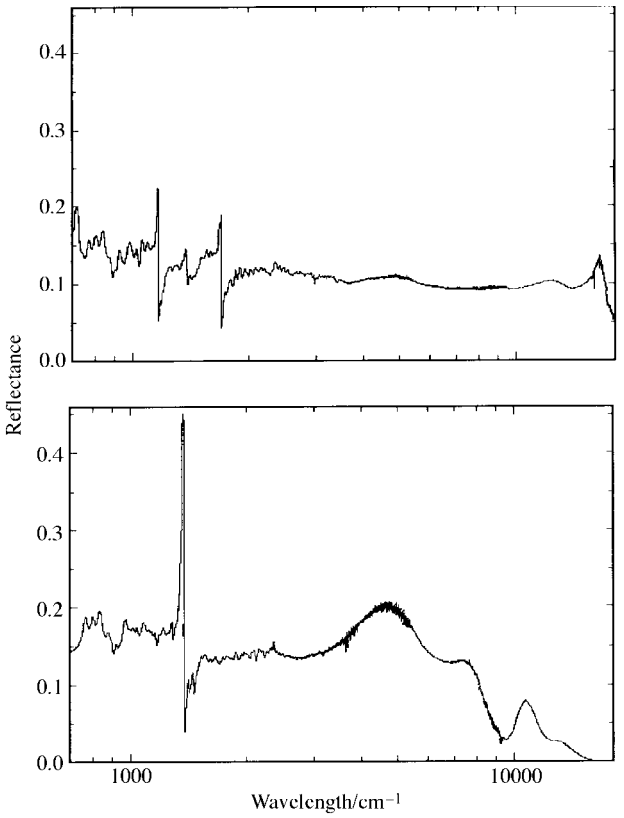

Fig. 1 Polarized reflectance spectra of (BEDT-TTF)$_2$[Pt(dts)$_2$] between 700 and 18000 cm^{-1}. Upper panel: electric vector perpendicular to the *b* crystallographic axis (stack axis). Lower panel: electric vector parallel to the *b* axis. Note the logarithmic wavenumber scale.

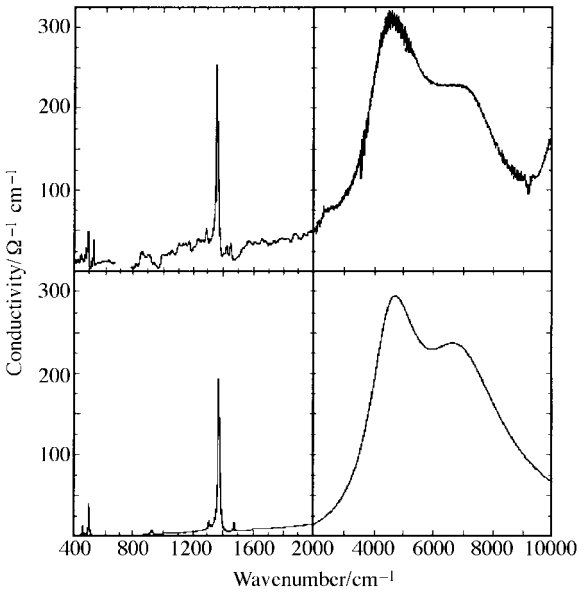

Fig. 2 Conductivity spectra of (BEDT-TTF)$_2$[Pt(dts)$_2$] between 400 and 10000 cm^{-1}, electric vector parallel to the *b* stack axis: (a) experimental spectrum, (b) calculated spectrum.

as appropriate for a semiconductor, and following standard procedures[13] for the high frequency extrapolation. The corresponding conductivity spectrum between 400 and 10000 cm^{-1} in the ∥ polarization is shown in the upper part of Fig. 2. For the 400–600 cm^{-1} region, where no microreflectance data are available, we obtained the unpolarized absorption spectrum of the powder. As is well known,[14] for very thin samples the IR absorption spectra can be considered proportional to the conductivity spectra. The intensities are normalized to the 1355 cm^{-1} band of the parallel conductivity spectrum. The two CT transitions show maximum conductivity at 4699 and 7006 cm^{-1}, and oscillator strengths of 0.33 and 0.37, respectively.

The Raman spectra of (BEDT-TTF)$_2$[Pt(dts)$_2$] powders are shown in Fig. 3, both at room temperature and at *ca.* 20 K.

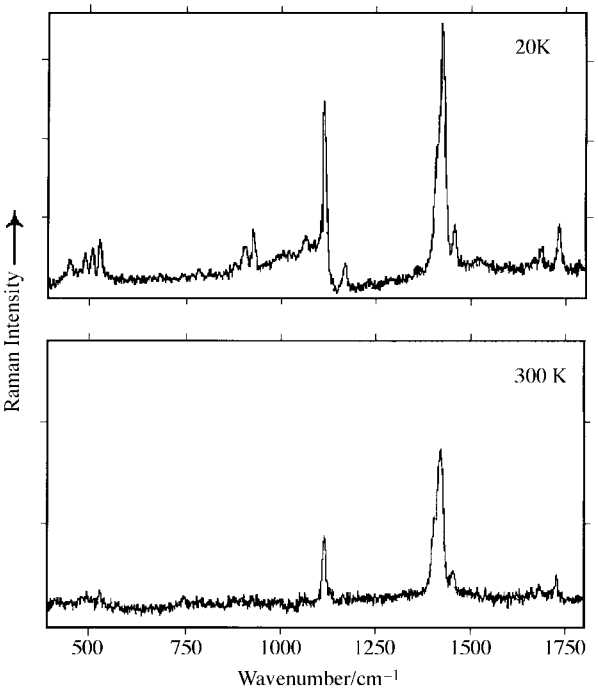

Fig. 3 Raman spectra of (BEDT-TTF)$_2$[Pt(dts)$_2$] between 400 and 1800 cm^{-1}. Upper panel: spectrum recorded at *ca.* 20 K. Lower panel: room temperature spectrum.

The use of higher laser power and a consequently better S/N ratio accounts for the greater number of bands observed in the low temperature spectrum in comparison to the room temperature spectrum. The room temperature Raman and IR vibrational data are collected in Table 1. The IR data of Fig. 2 are confirmed and complemented by the polarized absorption spectra of single crystals. The absorption spectra are not shown since the (BEDT-TTF)$_2$[Pt(dts)$_2$] crystals are rather thick and the most intense bands are distorted by absorbance saturation. The band assignment given in last column of Table 1 is straightforward given the IR polarization data and from a comparison with the spectra of (BEDT-TTF)$_2$[Mo_6O_{19}][15] and of K_2[Pt(dts)$_2$]·2H_2O (not reported here for the sake of brevity). The detailed assignement of BEDT-TTF modes is based on D_{2h} molecular symmetry, as usual for this molecule,[15] although the actual symmetry of the cation is D_2. From Table 1 we note that several IR bands in the ∥ polarization are assigned to molecular modes of a_g symmetry, and are associated with Raman bands of slightly higher wavenumber. From their wavenumber and polarization, these IR absorptions are easily recognized as arising from coupling between the molecular vibrations and the CT electrons (e–mv coupling), a well known phenomenon for CT crystals.[9,16] A more detailed analysis is presented in the next section.

Table 1 Room temperature IR and Raman wavenumbers (400–1800 cm^{-1}) of (BEDT-TTF)$_2$[Pt(dts)$_2$]

Raman	IR		
ν^a/cm^{-1}	ν^a/cm^{-1}	Pol.	Assignment[b]
453[c]w	448w	—	a_g ν_{10}
	478m	—	b_{1u} or b_{3u}
493vw			b_{1g} or b_{2g}
507[c]s	492ms	—	a_g ν_9
528w			[Pt(dts)$_2$]$^{2-}$
	530m	—	[Pt(dts)$_2$]$^{2-}$
	667w	⊥	b_{1u} ν_{33}
	683w	⊥	
	746s	⊥	[Pt(dts)$_2$]$^{2-}$
	781vw	⊥, ∥	
	785w	∥, ⊥	
	789vw	⊥, ∥	
	812w	∥	
	863s	⊥	[Pt(dts)$_2$]$^{2-}$
	876vs	⊥, ∥	[Pt(dts)$_2$]$^{2-}$
	887m	∥, ⊥	b_{2u} ν_{50}
904[c]w	897vs	∥, ⊥	a_g ν_7
	906s	∥, ⊥	
	926ms	∥, ⊥	[Pt(dts)$_2$]$^{2-}$
927[c]m			
	987w	∥	
	1008m	⊥	[Pt(dts)$_2$]$^{2-}$
	1026vs	⊥, ∥	b_{2u} ν_{47}
	1113w	⊥	
1115ms			[Pt(dts)$_2$]$^{2-}$
	1124vw	∥	[Pt(dts)$_2$]$^{2-}$
	1127m	⊥	[Pt(dts)$_2$]$^{2-}$
	1160vs	⊥	[Pt(dts)$_2$]$^{2-}$
	1162ms	∥	
	1167s	∥	
	1255w	⊥, ∥	
	1258ms	∥	
	1279vs	∥	a_g ν_5
	1318w	⊥	
1405(sh)			[Pt(dts)$_2$]$^{2-}$
1415(sh)			[Pt(dts)$_2$]$^{2-}$
1425vs	1355vs	∥	a_g ν_3
	1368vs	⊥	[Pt(dts)$_2$]$^{2-}$
	1394vs		
	1397vs	⊥	[Pt(dts)$_2$]$^{2-}$
	1410vs	⊥	b_{2u} ν_{45}
	1417vs	∥	[Pt(dts)$_2$]$^{2-}$
	1433m	⊥	
1455mw	1446vs	∥	a_g ν_2
	1452vw	⊥	b_{1u} ν_{27}
	1533w (br)	∥	
	1645mw	⊥	[Pt(dts)$_2$]$^{2-}$
	1678vs	⊥	[Pt(dts)$_2$]$^{2-}$
	1682w	∥	[Pt(dts)$_2$]$^{2-}$
	1718w	∥	[Pt(dts)$_2$]$^{2-}$
	1728w	∥	[Pt(dts)$_2$]$^{2-}$
1729mw			[Pt(dts)$_2$]$^{2-}$
	1732vs	⊥	[Pt(dts)$_2$]$^{2-}$
	1735(sh)	⊥	[Pt(dts)$_2$]$^{2-}$

[a]Qualitative relative intensities expressed as: vs, very strong; s, strong; ms, medium strong; m medium; mw, medium weak; w, weak; vw, very weak; sh, shoulder; br, broad. [b]Classification following assumed D_{2h} symmetry. The mode numbering is from ref. 21. [c]Exciting line: 632.8 nm.

3.2 Spectral analysis: on-site charge distribution and e–mv coupling

Analysis of BEDT-TTF bond distances[6] appears to indicate that in (BEDT-TTF)$_2$[Pt(dts)$_2$] the average charge (degree of ionicity, ρ) on each donor is +1. However, a more detailed scrutiny of the spectral data shows small but systematic deviations from full ionicity. Vibrational studies on several BEDT-TTF salts have shown that the degree of ionicity can be estimated by exploiting the almost linear dependence upon ρ of the wavenumbers of the a_g ν_2, ν_3 and ν_9 and b_{1u} ν_{27} modes.[17–19] The assignment of the b_{1u} ν_{27} mode is somewhat problematic, since only a very weak band at 1452 cm^{-1} is observed. Using this wavenumber and the room temperature wavenumbers of BEDT-TTF^0 and BEDT-TTF$^+$,[20,21] we estimate that $\rho = 0.89$. We anticipate that in the (BEDT-TTF)$_2$[Pt(dts)$_2$] crystal, the totally symmetric Raman modes of both donor and acceptor molecules may be perturbed by e–mv interactions, which involves the CT transition between BEDT-TTF and [Pt(dts)$_2$].[9] On the other hand, as discussed below, the perturbing effects on the Raman wavenumbers are fairly small. The weighted ratio of the ρ values obtained from the Raman wavenumbers of a_g ν_2, ν_3 and ν_9 modes, showing different behaviour *versus* ionicity,[18,19] yields $\rho = 0.91$. Therefore we can safely conclude that the degree of ionicity of (BEDT-TTF)$_2$[Pt(dts)$_2$] is *ca.* 0.9. This result confirms that there is direct CT interaction between BEDT-TTF and [Pt(dts)$_2$], as suggested above by the presence of two CT electronic transitions, and indicates that in the bis(dithiosquarate) salt the Pt(III) oxidation state is fairly close in energy to the stable Pt(II) oxidation state.

In the light of the above discussion, we can schematically represent the (BEDT-TTF)$_2$[Pt(dts)$_2$] stack by the sequence … $A^{1.8-}D^{0.9+}D^{0.9+}A^{1.8-}D^{0.9+}D^{0.9+}A^{1.8-}$…, where A represents the [Pt(dts)$_2$] acceptor and D the BEDT-TTF donor. There are two inversion centers in the stack, one between two neighbouring BEDT-TTF, and the other on the [Pt(dts)$_2$] anion.[6] The infinite chain can be thought of as built up by the repetition of trimeric DAD units. From this point of view, the (BEDT-TTF)$_2$[Pt(dts)$_2$] stack can be considered analogous to a trimerized segregated stack with inequivalent sites, such as in $Cs_2(TCNQ)_3$. In the latter crystals, the average charge on the TCNQ sites is not uniform, with two quasi-ionic TCNQs sandwiching a quasi-neutral TCNQ in a trimeric unit along the stack.[9] In such a case the TCNQ stack has developed a s-CDW whose amplitude is represented by the deviation of the average charge from the uniform charge or electron distribution along the sites. By analogy, we can consider the (BEDT-TTF)$_2$[Pt(dts)$_2$] stack as an intrinsic s-CDW stack. The amplitude of the s-CDW is represented by the deviation from uniformity of the electron distribution along the stack (two electrons are implied in the charge transfer over three sites). This quantity is directly proportional to the absolute value of the charge distribution, so we can interchangeably use the terms 'average value of the charge on the sites' and 'amplitude of the s-CDW'.

Following the above analogy, we can analyze the (BEDT-TTF)$_2$[Pt(dts)$_2$] optical spectra in terms of the semiempirical model already developed for $Cs_2(TCNQ)_3$.[9] The electronic structure of the stack is described in terms of a limited set of basis functions for the infinite chain, disregarding the higher energy functions. The lowest energy basis function is:

$$\Phi^0 = \prod_i |D_i^+ A_i^{2-} D_i^+\rangle = \prod_i \Psi_i \quad (1)$$

the product running over all the N trimeric units of the chain. We then have $2N$ functions corresponding to the transfer of one electron from the central molecule to the lateral left and right donor molecules within the trimer, $|D_i^0 A_i^- D_i^+\rangle \prod_{j\neq i} \Psi_j$ and $|D_i^+ A_i^- D_i^0\rangle \prod_{j\neq i} \Psi_j$. Each pair is degenerate, and, exploiting both the translational and point symmetry, we combine them to give the following $\boldsymbol{k}=0$ wavefunctions:

$$\Phi^{\text{intra}+} = N^{-1/2} \sum_i \left\{ 2^{-1/2} \left(|D_i^0 A_i^- D_i^+\rangle \prod_{j\neq i} \Psi_j + |D_i^+ A_i^- D_i^0\rangle \prod_{j\neq i} \Psi_j \right) \right\}$$

$$\Phi^{\text{intra}-} = N^{-1/2} \sum_i \left\{ 2^{-1/2} \left(|D_i^0 A_i^- D_i^+\rangle \prod_{j\neq i} \Psi_j - |D_i^+ A_i^- D_i^0\rangle \prod_{j\neq i} \Psi_j \right) \right\} \quad (2)$$

where the + and − combinations correspond to states which are symmetric and antisymmetric with respect to the inversion on the A site. We consider also the left and right transfer of one electron between two trimers, that is, between two adjacent BEDT-TTF molecules belonging to different trimers. Again, the two functions combine in-phase and out-of-phase to give the following $\boldsymbol{k}=0$ states:

$$\Phi^{\text{inter}+} = N^{-1/2} \sum_i \left\{ 2^{-1/2} \left(|D_i^+ A_i^{2-} D_i^0 D_{i+1}^{2+} A_{i+1}^{2-} D_{i+1}^+\rangle \prod_{j\neq i,\ i+1} \Psi_j + |D_i^+ A_i^{2-} D_i^{2+} D_{i+1}^0 A_{i+1}^{2-} D_{i+1}^+\rangle \prod_{j\neq i,\ i+1} \Psi_j \right) \right\}$$

$$\Phi^{\text{inter}-} = N^{-1/2} \sum_i \left\{ 2^{-1/2} \left(|D_i^+ A_i^{2-} D_i^0 D_{i+1}^{2+} A_{i+1}^{2-} D_{i+1}^+\rangle \prod_{j\neq i,\ i+1} \Psi_j - |D_i^+ A_i^{2-} D_i^{2+} D_{i+1}^0 A_{i+1}^{2-} D_{i+1}^+\rangle \prod_{j\neq i,\ i+1} \Psi_j \right) \right\} \quad (3)$$

By symmetry, the Φ^0 basis function mixes only to $\Phi^{\text{intra}+}$ and $\Phi^{\text{inter}+}$, so that the eigenfunctions of the Hamiltonian can be written as:

$$\begin{aligned} \Psi^{(1)} &= a_0\Phi^0 + a_1\Phi^{\text{intra}+} + a_2\Phi^{\text{inter}+} \\ \Psi^{(2)} &= b_0\Phi^0 + b_1\Phi^{\text{intra}+} \\ \Psi^{(3)} &= c_0\Phi^0 + c_1\Phi^{\text{inter}+} \\ \Psi^{(4)} &= \Phi^{\text{intra}-} \\ \Psi^{(5)} &= \Phi^{\text{inter}-} \end{aligned} \quad (4)$$

The only electric dipole allowed transitions are the $|\Psi^{(4)}\rangle \leftarrow |\Psi^{(1)}\rangle$ and the $|\Psi^{(5)}\rangle \leftarrow |\Psi^{(1)}\rangle$ (from the symmetric ground state to the antisymmetric states), with dipole moment $\mu_{\text{CT}}^{\text{intra}} = N^{-1/2} a_1 e d_1$ and $\mu_{\text{CT}}^{\text{inter}} = N^{-1/2} a_2 e d_2$, respectively, where e is the electron charge, and d_1, d_2 are the distances between molecules within the trimer and between trimers, respectively.

To account for the coupling between CT electrons and molecular vibrations (e–mv coupling),[9,16] we have first to introduce the purely vibrational part. We limit the attention to the totally symmetric (a_g) modes of the donor and acceptor molecules, as these are the only modes which can couple to electrons *via* the modulations of the on-site energies.[16] As for the electronic part, the αth a_g molecular normal coordinate $q_{i,\alpha}^{(l)}$ and $q_{i,\alpha}^{(r)}$ of the left and right BEDT-TTF in the ith trimer are combined in- and out-of-phase: $S_{i,\alpha} = 2^{-1/2}(q_{i,\alpha}^{(l)} + q_{i,\alpha}^{(r)})$ and $A_{i,\alpha} = 2^{-1/2}(q_{i,\alpha}^{(l)} - q_{i,\alpha}^{(r)})$. Denoting $Q_{i,\beta}$ as the βth a_g normal mode of the [Pt(dts)$_2$] moiety, we have the following $\boldsymbol{k}=0$ normal coordinates for the chain made up of N trimers:

$$\begin{aligned} S_\alpha &= N^{-1/2} \sum_i S_{i,\alpha} \\ A_\alpha &= N^{-1/2} \sum_i A_{i,\alpha} \\ Q_\beta &= N^{-1/2} \sum_i Q_{i,\beta} \end{aligned} \quad (5)$$

Simple symmetry arguments show that the S_α and Q_β modes are Raman active, whereas the out-of-phase combinations of BEDT-TTF modes, A_α, are IR active. In terms of the above normal coordinates, the linear e–mv Hamiltonian can be written as:[9]

$$H_{\text{emv}} = \sum_{i,\alpha} \sqrt{\omega_\alpha} g_\alpha \{ (\boldsymbol{n}_{i,\text{l}} + \boldsymbol{n}_{i,\text{r}}) S_\alpha + (\boldsymbol{n}_{i,\text{l}} - \boldsymbol{n}_{i,\text{r}}) A_\alpha \} + \sum_{i,\beta} \sqrt{2\omega_\beta} g_\beta \boldsymbol{n}_{i,\text{c}} Q_\beta \quad (6)$$

where ω_α and ω_β are the unperturbed vibrational wavenumbers of BEDT-TTF and [Pt(dts)$_2$], respectively, and $\boldsymbol{n}_{\text{i,l}}$, $\boldsymbol{n}_{\text{i,r}}$ and $\boldsymbol{n}_{\text{i,c}}$ are the electron number occupation operators for left, right and central trimer sites. The linear e–mv coupling constants g_α and g_β are defined as $g_\alpha = (\partial\varepsilon_{\text{l,r}}/\partial q_\alpha^{\text{l,r}})_0$ and $g_\beta = (\partial\varepsilon_{\text{c}}/\partial q_\beta)_0$ for lateral and central molecules within the trimer, $\varepsilon_{\text{l,r}}$ and ε_{c} being the corresponding on-site energies.

Following ref. 16, H_{emv} is treated in the Herzberg–Teller approach, and the e–mv perturbed wavenumbers, Ω_α, are obtained by diagonalizing the 'force constants' matrix $\boldsymbol{F}$, whose elements in the A_α subspace are:

$$\begin{aligned} F(A_\alpha, A_\alpha) &= \omega_\alpha^2 - 2g_\alpha^2\omega_\alpha \left(\frac{4|\mu_{\text{CT}}^{\text{inter}}|^2}{e d_2^2 \omega_{\text{CT}}^{\text{inter}}} + \frac{|\mu_{\text{CT}}^{\text{intra}}|^2}{e d_1^2 \omega_{\text{CT}}^{\text{intra}}} \right) \\ F(A_\alpha, A_{\alpha'}) &= -2g_\alpha g_{\alpha'} \sqrt{\omega_\alpha \omega_{\alpha'}} \left(\frac{4|\mu_{\text{CT}}^{\text{inter}}|^2}{e d_2^2 \omega_{\text{CT}}^{\text{inter}}} + \frac{|\mu_{\text{CT}}^{\text{intra}}|^2}{e d_1^2 \omega_{\text{CT}}^{\text{intra}}} \right) \end{aligned} \quad (7)$$

where the G_α are connected to the e–mv coupling constants through $G_\alpha = \sum_{\alpha'} L_{\alpha',\alpha} g_{\alpha'}$, $L_{\alpha',\alpha}$ being the elements of the unitary matrix which diagonalizes the force constants matrix $\boldsymbol{F}$. Finally, we apply linear response theory to obtain the following expression for the wavenumber dependent conductivity along the stack axis:

$$\sigma(\omega) = -\frac{i\omega N_t}{\hbar} \left\{ \chi_{\text{CT}}^{\text{intra}}(\omega) \left[1 - \frac{\sum_\alpha \lambda_\alpha^{\text{intra}} \Omega_\alpha^2}{\Omega_\alpha^2 - \omega^2 - i\omega\gamma_\alpha} \right] + \chi_{\text{CT}}^{\text{inter}}(\omega) \left[1 + \frac{\sum_\alpha \lambda_\alpha^{\text{inter}} \Omega_\alpha^2}{\Omega_\alpha^2 - \omega^2 - i\omega\gamma_\alpha} \right] \right\} \quad (8)$$

where N_t is the number of trimers per unit volume, $\chi_{\text{CT}}^{\text{intra}}$ and $\chi_{\text{CT}}^{\text{inter}}$ are the CT electronic susceptibilities $\chi_{\text{CT}}(\omega) = 2|\mu_{\text{CT}}|^2 \omega_{\text{CT}}/(\omega_{\text{CT}}^2 - \omega^2 - i\omega\gamma_{\text{CT}})$, and the λs are connected to the e–mv coupling constants through:

$$\begin{aligned} \lambda_\alpha^{\text{intra}} &= \frac{2G_\alpha^2}{e\Omega_\alpha^2 d_1} \left(\frac{2|\mu_{\text{CT}}^{\text{inter}}|^2}{e d_2 \omega_{\text{CT}}^{\text{inter}}} - \frac{|\mu_{\text{CT}}^{\text{intra}}|^2}{e d_1 \omega_{\text{CT}}^{\text{intra}}} \right) \\ \lambda_\alpha^{\text{inter}} &= \frac{4G_\alpha^2}{e\Omega_\alpha^2 d_2} \left(\frac{2|\mu_{\text{CT}}^{\text{inter}}|^2}{e d_2 \omega_{\text{CT}}^{\text{inter}}} - \frac{|\mu_{\text{CT}}^{\text{intra}}|^2}{e d_1 \omega_{\text{CT}}^{\text{intra}}} \right) \end{aligned} \quad (9)$$

Eqn. (8) shows that the conductivity along the stack axis presents, in addition to the two CT transitions, a series of

e–mv induced bands associated with the a_g modes of BEDT-TTF. In order to evaluate Re[$\sigma(\omega)$], we derive $|\mu_{CT}^{intra}|^2$, $|\mu_{CT}^{inter}|^2$ and the corresponding damping constants γ_{CT}^{intra}, γ_{CT}^{inter} from the experimental spectra, and d_1, d_2, from the crystal structure.[6] The unperturbed wavenumbers ω_α are obtained by linear interpolation from the wavenumbers of the Raman active a_g modes of neutral and fully ionic BEDT-TTF, assuming 0.9 as average charge on the molecule. Furthermore, we adopt the same values of the e–mv coupling constants as recently estimated from (BEDT-TTF)$_2$[Mo_6O_{19}] optical spectra,[15] adjusted to take into account the different molecular charge.[16] The only adjustable parameters in the calculations are then the damping constants of the vibrational modes, γ_α. The calculated conductivity spectrum is shown in the lower part of Fig. 2. The good agreement with the experimental spectrum (Fig. 2, upper part), particularly in terms of the wavenumber and the intensity of the e–mv induced IR bands, confirms the validity of the adopted interpretative scheme and the transferability of BEDT-TTF e–mv coupling constants. We note that such an agreement can be obtained only by associating the inter- and intra-trimer CT transitions to the 4699 and 7006 cm^{-1} bands, respectively.

Turning our attention to the Raman active modes, S_α and Q_α, as it is already known from the $Cs_2(TCNQ)_3$ system, the wavenumbers of these modes are affected by e–mv coupling.[9] To obtain a rough estimate of the e–mv wavenumber shift of the Raman modes, we introduce a further simplification into the model, considering an isolated (BEDT-TTF)[Pt(dts)$_2$](BEDT-TTF) trimer. Following this approach it is readily seen that in the present case, given the intratrimer CT transition at 7006 cm^{-1} is relatively far from the vibrational region, the effect of e–mv perturbation on the Raman wavenumbers will be rather small, amounting to <5 cm^{-1} for the most strongly coupled modes. For this reason the s-CDW amplitude estimated above from the a_g Raman modes of BEDT-TTF is approximately the same (0.9) as that evaluated from the unperturbed modes. For the isolated trimer approximation, the s-CDW amplitude can be estimated from the intensity of the intra-trimer CT transition,[22] and a value of $\rho \cong 0.9$ is again obtained.

3.3 Temperature and pressure effects

The temperature and pressure evolution of the IR and Raman spectra of (BEDT-TTF)$_2$[Pt(dts)$_2$] were studied to investigate possible changes in the s-CDW amplitude and the occurrence of phase transitions. We recorded Raman spectra down to 20 K (Fig. 3 upper panel) and IR spectra down to 77 K. The IR and Raman spectra do not display appreciable changes with temperature, showing that the s-CDW amplitude and the stack structure is essentially the same both at room and low temperature. Only two minor effects are observed in the IR spectra of (BEDT-TTF)$_2$[Pt(dts)$_2$] upon lowering the temperature to 77 K. One is the appearance of a weak band (‖ polarization) at 1174 cm^{-1}, and the other is the shift of the very weak band at 1124 cm^{-1} (‖ polarization) assigned to [Pt(dts)$_2$]$^{2-}$ anion which softens down to 1121 cm^{-1}.

Quite pronounced spectral variations, indicative of the occurrence of phase transitions, are, however, observed by applying pressure. Fig. 4 shows the evolution with pressure of the IR spectra (‖ polarization) of (BEDT-TTF)$_2$[Pt(dts)$_2$] in the regions 1100–1200 and 1375–1445 cm^{-1}. We can recognize two main spectral variations, one in the range 1–1.6 GPa and the other in the range 2.2–2.5 GPa. Full reversibility of the spectra is observed by releasing the pressure to ambient. We associate the two spectral variations to two distinct phase transitions. The first phase transition is characterized by the appearance of some IR absorption bands in the polarization parallel to the stack axis. The three bands at 1124, 1177 and 1412 cm^{-1} (Fig. 4) appearing above 1.0 GPa cannot be

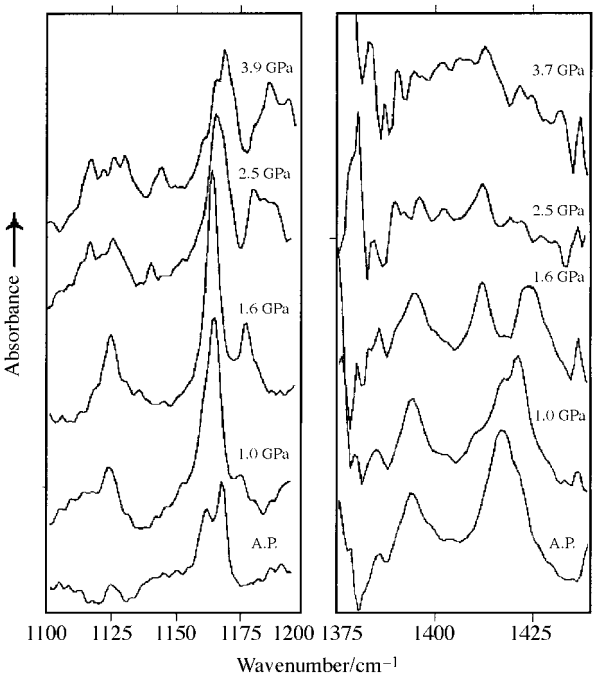

Fig. 4 Pressure dependence of (BEDT-TTF)$_2$[Pt(dts)$_2$] absorption spectra (electric vector parallel to the *b* stack axis) in the 1100–1200 and 1375–1445 cm^{-1} spectral regions. The absorbance scale is in arbitrary units, and the spectra are offset for clarity. A.P. stands for ambient pressure.

assigned to *ungerade* IR active modes of BEDT-TTF$^+$ or [Pt(dts)$_2$]$^{2-}$ moieties, and are attributed to a_g modes of the [Pt(dts)$_2$]$^{2-}$ anion. The assignments follow from a comparison with the Raman spectra of (BEDT-TTF)$_2$[Pt(dts)$_2$] and K_2[Pt(dts)$_2$], where a_g modes with similar wavenumber are observed at ambient pressure. While other totally symmetric a_g modes appear in the IR spectra above 1.0 GPa, we focus our attention on the above three modes, as they occur in spectral regions free from the overlapping of other fundamental modes. These three IR absorption bands are attributed to bands of vibronic origin, following a stack distortion.[16,23] If the stack is not distorted, the [Pt(dts)$_2$]$^{2-}$ anion would lie on an inversion centre and the a_g modes would be IR forbidden; on the other hand, when the inversion centre is lost, the a_g modes become IR active, borrowing intensity from the nearby CT transition between BEDT-TTF and the [Pt(dts)$_2$] anion. Therefore the first phase transition likely involves a stack distortion. The spectral variations occurring above 2.2 GPa are mainly splitting and/or broadening of several IR bands, both in parallel (Fig. 4) and perpendicular polarization. We attribute these variations to Davydov splittings,[24] possibly due to the doubling of the unit cell. Further speculation on the nature of this second phase transition cannot be advanced, also because sample decomposition prevents the collection of high pressure Raman data. For the same reason we cannot ascertain the variation of the s-CDW amplitude with pressure, the IR data merely suggesting that there is no drastic change.

4 Discussion and conclusions

The crystal structure of (BEDT-TTF)$_2$[Pt(dts)$_2$], where (BEDT-TTF)$_2$ dimers are separated by [Pt(dts)$_2$] counter ions, is rather unusual among BEDT-TTF salts. Previous studies[6,7] suggested that (BEDT-TTF)$_2$ dimers bear a dipositive charge. This would imply that the (BEDT-TTF)$_2$ dimers do not appreciably interact with counter ions, as for example in crystals of (BEDT-TTF)$_2$[Mo_6O_{19}].[15] The particular stack structure of (BEDT-TTF)$_2$[Pt(dts)$_2$] was ascribed to the similarity of the cation and anion molecular shapes, *i.e.*, to steric

factors summing up to the Coulomb forces.[7] Here, however, we have shown that the above picture is not correct, and that the stack structure is indeed stabilized by the CT interaction both between BEDT-TTF ions *and* between BEDT-TTF and $[Pt(dts)_2]$. The proximity of the two CT transitions (Fig. 1) is probably the reason why the latter interaction was not registered in previous studies.[7] On the other hand, this proximity and the consequent mixing invalidates the view of the $(BEDT\text{-}TTF)_2[Pt(dts)_2]$ stack as a mixed stack, with the $(BEDT\text{-}TTF)_2$ supermolecule acting as an electron donor. As shown by Fig. 2, a model[9] analogous to that developed for segregated stacks with on-site CDW (inequivalent sites) is able to properly reproduce the optical data. Following the classification of Robin and Day,[25,26] $(BEDT\text{-}TTF)_2[Pt(dts)_2]$ can thus be considered a class II system, *i.e.* a localized mixed-valence system.

A detailed analysis of the optical spectra has allowed us to unambiguously demonstrate that the average charge on BEDT-TTF molecules is ≈ 0.9. This datum emerges consistently from the wavenumber of the IR vibrational modes, as well as from that of the slightly perturbed Raman modes, and from the intensity of the CT transitions. The corresponding average charge of -1.8 on $[Pt(dts)_2]$ counter ion suggests that the unstable Pt(III) oxidation state is not too far in energy from the Pt(II) ground state. Indeed, cyclic voltammetry data have already shown that the one electron redox potentials of $BEDT\text{-}TTF^+$ and $[Pt(dts)_2]^-$ are 0.59 and 0.54 V, respectively.[6] Of course, we cannot exclude that the dominant role in the redox processes is played by the dithiosquarate ligand rather than by the metal centre. On the other hand, and contrary to what might have been expected, the s-CDW amplitude of $(BEDT\text{-}TTF)_2[Pt(dts)_2]$ is little affected by temperature or pressure variations. Under pressure the system readily undergoes a stack distortion, with a b-CDW overlapping the intrinsic s-CDW. A further pressure increase probably favours interstack interactions, with consequent changes in the unit cell.

Since the synthesis of $(BEDT\text{-}TTF)_2[Pt(dts)_2]$,[6] several other salts of $[M(dts)_2]$ (M = Pt, Pd, Au) with BEDT-TTF and its selenium isologue, bis(ethylenedithio)tetraselenafulvalene (BEDT-TSF), have been prepared and characterized.[7] With one exception, they all have a similar stack structure to that of $(BEDT\text{-}TTF)_2[Pt(dts)_2]$, and are semiconductors or insulators. $(BEDT\text{-}TSF)[Au(dts)_2]$ has low resistivity, but along a lateral direction involving Se–Se and S–S contacts between BEDT-TSF molecules in different stacks. Rather than to the 'mixed stack' structure of the complexes, we attribute the semiconducting behaviour to the localized mixed-valence character, most probably due to high on-site electron repulsions on the $[M(dts)_2]$ sites.

Acknowledgements

We gratefully acknowledge support by the Italian National Research Council (CNR) within its 'Progetto Finalizzato Materiali Speciali per Tecnologie Avanzate II', and by the Ministry of University and Scientific and Technological Research (MURST). One of us (C.B.) thanks Mr F. Federici for technical assistance and CNR for financial support. We gratefully thank Professor R. Bozio (Padova University) for allowing us to measure the Raman spectra in his laboratory, and M. Zanetti for technical support. We also thank Dr A. Painelli for many helpful discussions.

References

1 T. Ishiguro and K. Yamaji, *Organic Superconductors*, Springer-Verlag, Berlin, 2nd edn., 1998.
2 A. Kobayashi, T. Udagawa, H. Tomita, T. Naito and H. Kobayashi, *Chem. Lett.*, 1993, 2179.
3 R. H. Mckenzie, *Science*, 1997, **278**, 820.
4 H. Kobayashi, H. Tomita, T. Naito, A. Kobayashi, F. Sakai, T. Watanabe and P. Cassoux, *J. Am. Chem. Soc.*, 1996, **118**, 368; A. Kobayashi, T. Idagawa, H. Tomita, T. Naito and H. Kobayashi, *Chem. Lett*., 1993, 2179; M. Kurmoo, A. W. Graham, P. Day, J. Coles, M. B. Hursthouse, J. L. Caulfield, J. Singleton, F. L. Pratt, W. Hayes and L. Ducasse, *J. Am. Chem. Soc.*, 1995, **117**, 12209; C. Bellitto, M. Bonamico, V. Fares, F. Federici, G. Righini, M. Kurmoo and P. Day, *Chem. Mater.*, 1995, **7**, 1475.
5 A. E. Underhill, *J. Mater. Chem.*, 1992, **2**, 1; T. Nakamura, T. Agutagawa, K. Honda, A. E. Underhill, A. T. Coombers and R. H. Friend, *Nature*, 1998, **394**, 159.
6 C. Bellitto, M. Bonamico, V. Fares and P. Serino, *Inorg. Chem.*, 1996, **35**, 4070.
7 H. Tanaka, A. Kobayashi and H. Kobayashi, *Bull. Chem. Soc. Jpn*., 1997, **70**, 3137.
8 Z. G. Soos and D. J. Klein, in *Molecular Association*, ed. R. Foster, Academic Press, London, 1975, vol. 1, ch. 1.
9 A. Painelli, C. Pecile and A. Girlando, *Mol. Cryst. Liq. Cryst.*, 1986, **134**, 1.
10 D. Coucouvanis, D. G. Holah and F. J. Hollander, *Inorg. Chem.*, 1975, **14**, 2657.
11 G. J. Piermarini, S. Block, J. D. Barret and R. A. Forman, *J. Appl. Phys.*, 1975, **46**, 2744.
12 T. Hasegawa, S. Kagoshima, T. Mochida, S. Sugiura and Y. Iwasa, *Solid State Commun.*, 1997, **103**, 489.
13 F. Wooten, *Optical Properties of Solids*, Academic Press, New York, 1972.
14 J. C. Decius and R. M. Hexter, *Molecular Vibrations in Crystals*, McGraw-Hill, New York, 1977, p. 190.
15 G. Visentini, M. Masino, C. Bellitto and A. Girlando, *Phys. Rev. B:Condens. Matter*, 1998, **58**, 9460.
16 A. Painelli and A. Girlando, *J. Chem. Phys*., 1986, **84**, 5655.
17 J. Moldenhauer, Ch. Horn, K. I. Pokhodnia, D. Schweitzer, I. Heinen and H. J. Keller, *Synth. Met.*, 1993, **60**, 31.
18 H. H. Wang, J. R. Ferraro, J. M. Williams, U. Geiser and J. A. Schlueter, *J. Chem. Soc., Chem. Commun.*, 1994, 1893.
19 H. H. Wang, A. M. Kini and J. M. Williams, *Mol. Cryst. Liq. Cryst.*, 1996, **284**, 211.
20 M. E. Kozlov, K. I. Pokhodnia and A. A. Yurchenko, *Spectrochim. Acta*, *Part A*, 1989, **45**, 437.
21 J. E. Eldridge, C. C. Homes, J. M. Williams, A. M. Kini and H. H. Wang, *Spectochim. Acta*, *Part A*, 1995, **51**, 947.
22 A. Painelli and A. Girlando, *J. Chem. Phys.*, 1987, **87**, 1705.
23 C. Pecile, A. Painelli and A. Girlando, *Mol. Cryst. Liq. Cryst.*, 1989, **171**, 69.
24 G. Turrell, *Infrared and Raman Spectra of Crystals*, Academic Press, London, 1972.
25 M. B. Robin and P. Day, *Adv. Inorg. Chem. Radiochem.*, 1967, **10**, 247.
26 P. Delhaes, P. Day and G. C. Papavassiliou, *Lower-Dimensional Systems and Molecular Electronics*, ed. R. M. Metzger, *NATO ASI Ser., Ser. B*, 1990, **248**, 43.

Paper 9/01589B